

# Role of cross-shell excitations in the reaction $^{54}\text{Fe}(\vec{d}, p)^{55}\text{Fe}$

M. Mahgoub<sup>1</sup>, R. Krücken<sup>1</sup>, Th. Faestermann<sup>1</sup>, A. Bergmaier<sup>2</sup>, D. Bucurescu<sup>3</sup>, R. Hertenberger<sup>4</sup>, Th. Kröll<sup>1</sup>, H.-F. Wirth<sup>1,4</sup>, and A. F. Lisetskiy<sup>5,6</sup>

<sup>1</sup> Physik Department, Technische Universität München, D-85748 Garching, Germany

<sup>2</sup> Institut für Angewandte Physik und Messtechnik, Universität der Bundeswehr München, D-85577 Neubiberg, Germany

<sup>3</sup> Horia Hulubei National Institute of Physics and Nuclear Engineering (IFIN-HH), R-77125 Bucharest, Romania

<sup>4</sup> Department für Physik, Ludwig Maximilians Universität München, D-85748 Garching, Germany

<sup>5</sup> Gesellschaft für Schwerionenforschung, D-64291 Darmstadt, Germany

<sup>6</sup> Department of Physics, University of Arizona, Tucson, AZ 85721, USA

Received: date / Revised version: date

**Abstract.** The reaction  $^{54}\text{Fe}(\vec{d}, p)^{55}\text{Fe}$  was studied at the Munich Q3D spectrograph with a 14 MeV polarized deuteron beam. Excitation energies, angular distributions and analyzing powers were measured for 39 states up to 4.5 MeV excitation energy. Spin and parity assignments were made and spectroscopic factors deduced by comparison to DWBA calculations. The results were compared to predictions by large scale shell model calculations in the full pf-shell and it was found that reasonable agreement for energies and spectroscopic factors below 2.5 MeV could only be obtained if up to 6 particles were allowed to be excited from the  $f_{7/2}$  orbital into  $p_{3/2}$ ,  $f_{5/2}$ , and  $p_{1/2}$  orbitals across the  $N = 28$  gap. For levels above 2.5 MeV the experimental strength distribution was found to be significantly more fragmented than predicted by the shell model calculations.

**PACS.** 2.1.10.Jx, 21.10.Pc, 21.60.Cs, 25.45.Hi, 27.40.+z

## 1 Introduction

In the simplest spherical shell model approach the  $N = Z = 28$  nucleus  $^{56}\text{Ni}$  has the properties of a doubly-magic core. However, evidence for the softness of the  $^{56}\text{Ni}$  core has been obtained experimentally [1] and theoretically [2]. With the availability of more computing power and the development of the new effective interaction GXPF1 for the pf-shell [3] core excitations were found to play a significant role in the structure of nuclei in the vicinity of  $^{56}\text{Ni}$ [4]. Experimental evidence for the crucial role of cross-shell excitations for the yrast spectra was, for example, reported in  $^{58}\text{Cu}$  [5]. The stability of the magic number 28 is also of astrophysical importance, *e.g.* for the electron capture rates in supernova explosions (see *e.g.* Ref. [6]).

The current paper reports on a precision study of the excited states of  $^{55}\text{Fe}$  using the  $^{54}\text{Fe}(\vec{d}, p)^{55}\text{Fe}$  reaction. While this reaction has been performed several times in the past [7,8,9], those studies had limited energy resolution and sensitivity and therefore, spectroscopic factors and definite spin assignments were obtained only for a limited number of excited states. Those previous results were typically compared to shell model calculations that assumed a good  $^{56}\text{Ni}$  core and thus the sensitivity to cross-shell excitations was not tested.

The excellent energy resolution and sensitivity of the Munich Q3D magnetic spectrograph used in this study enabled the discovery of several new states and the determination of spins for a number of known states. For many states spectroscopic factors were determined for the first time. The data are compared to the results of large scale shell model calculations using the GXPF1 effective interaction. Reasonable agreement for energies and spectroscopic factors was achieved for states up to about 2.5 MeV when at least 6-particle 6-hole (6p-6h) excitations across the  $N=28$  shell gap were taken into account, while the experimental results could not be satisfactory reproduced if less than six particles are promoted across the shell gap. Thus, the results of our study clearly demonstrate the importance of  $^{56}\text{Ni}$  core excitations for  $^{54}\text{Fe}$  and  $^{55}\text{Fe}$ .

## 2 Experimental Details

The  $^{54}\text{Fe}(\vec{d}, p)^{55}\text{Fe}$  reaction was studied by bombarding a  $100\mu\text{g}/\text{cm}^2$  thick 94.6% isotopically enriched self supporting  $^{54}\text{Fe}$  target with polarized deuterons from a Stern-Gerlach polarized ion source [10] and accelerated to 14

MeV by the MLL<sup>1</sup> MP-Tandem Van de Graaff accelerator. The reaction products were analyzed with the Munich Q3D spectrograph [11] and then detected in a 1 m long cathode strip focal-plane detector [12,13] with  $\Delta E$ - $E_{rest}$  particle identification and position determination. The acceptance solid angle of the spectrograph was 11.7 msr (horizontally 54 mrad), except for the most forward angle (5°) where it was 5.7 msr. Typical beam currents were around 0.5  $\mu\text{A}$  on target.

Spectra were measured at 8 angles between 5° and 40° in 5° steps plus one measurement at 50°. For each angle six spectra were collected, for 3 different magnetic settings, covering the excitation energy range from 0 to  $\approx 4.5$  MeV and for spin-up and spin-down polarization of the deuteron beam, respectively. Figure 1 shows Q3D spectra for those settings taken at an angle of 30°. The overall FWHM energy resolution was around 7 keV, being mostly determined by the target thickness. The spectra were essentially background free. All runs were normalized to the beam current integrated by a Faraday cup placed behind the target. The spectra were calibrated by using the energies of those states in  $^{55}\text{Fe}$  that were known to better than 1 keV [8]. In the energy range from 3.0 to 4.5 MeV only three levels with sufficient energy are known at 3072.0, 3108.7, 3552.3 keV. However, as will be discussed below, there are four energy peaks previously assigned to  $^{55}\text{Fe}$  excitation energies at 3285, 3860, 4123, and 4372 keV which actually result from the contaminant reaction  $^{56}\text{Fe}(d,p)^{57}\text{Fe}$  present in this energy range, enabling an accurate energy calibration.

Differential reaction cross-sections for each angle were obtained by averaging the cross-sections obtained for spin-up ( $\frac{d\sigma}{d\Omega} \uparrow$ ) or spin-down ( $\frac{d\sigma}{d\Omega} \downarrow$ ) polarized beam. In addition to determine angular distributions, the polarized beam with a polarization of  $p = 0.65$  enabled calculating the analyzing power at each angle using the relation

$$A_y = \frac{2}{3p} \cdot \frac{\frac{d\sigma}{d\Omega} \uparrow - \frac{d\sigma}{d\Omega} \downarrow}{\frac{d\sigma}{d\Omega} \uparrow + \frac{d\sigma}{d\Omega} \downarrow}. \quad (1)$$

### 3 Results

In total 39 levels in  $^{55}\text{Fe}$  were observed in the energy range from 0 to 4450 keV, of which 6 levels are observed for the first time. For the other levels various amounts of information were available ranging from only the energy, a tentative or firm spin assignment to spectroscopic factors in some cases.

For five states that were previously assigned to  $^{55}\text{Fe}$  at 2015, 3285, 3860, 4123, and 4372 keV we could show that the observed lines actually belong to known levels in  $^{57}\text{Fe}$  at energies of 366, 1627, 2220, 2456, and 2758 keV. The lines resulted from the 5.1 %  $^{56}\text{Fe}$  component in our target. We proved the assignment to  $^{57}\text{Fe}$  by comparing the spectra for the  $(d,p)$  reaction from our 94.6% isotopically enriched  $^{54}\text{Fe}$  target with those obtained with a 99.9%

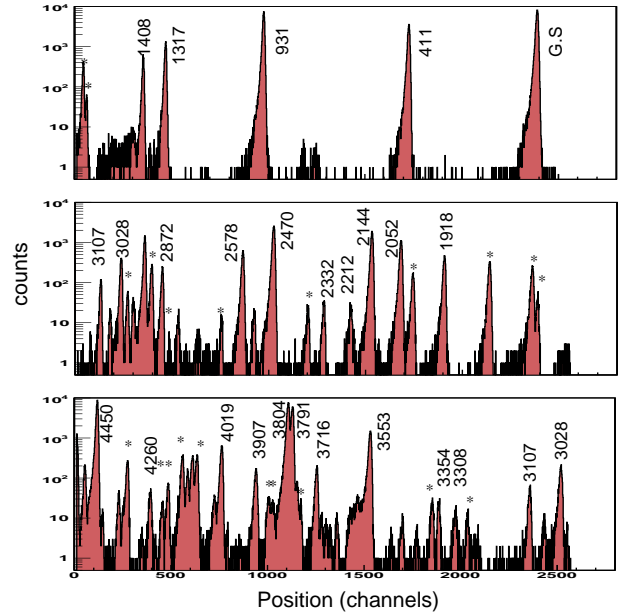


**Fig. 1.** Focal plane spectra of the Q3D observed at 30° with spin-up polarized deuteron beam for the reaction  $^{54}\text{Fe}(\vec{d},p)^{55}\text{Fe}$ . Magnetic field settings were chosen such that excitation energies of 600 keV (top), 2200 keV (middle), and 3600 keV (bottom) were centered on the Q3D focal plane. Energies for some levels, as obtained in this work, are given in keV. Lines marked with \* are from the  $^{56}\text{Fe}$  impurities in the target.

isotopically enriched  $^{56}\text{Fe}$  target under exactly same experimental conditions. The assignment of those levels to  $^{55}\text{Fe}$  [8,9,14,15] was based on transfer experiments that used targets with less than 95%  $^{54}\text{Fe}$  isotopic enrichment and thus lines of  $^{57}\text{Fe}$  would be expected in the spectra. However, we did not find any note in the original work that a direct comparison was performed with a pure  $^{56}\text{Fe}$  target in order to identify contributions from the  $^{56}\text{Fe}(d,p)$  reaction in the spectra. We are therefore confident that the levels at 2015, 3285, 3860, 4123, and 4372 keV do not exist in  $^{55}\text{Fe}$ .

Angular distributions and analyzing powers are shown in figs. 2-10. Total angular momenta and parities  $J^\pi$  were deduced by comparison with results of distorted-wave Born approximation (DWBA) calculations with the code CHUCK3[16]. Three different sets of optical model parameters were used, which are summarized in table 1.

The non-locality parameter  $\beta$  for the particles mentioned in tab. 1 is taken from Ref. [19]. The finite-range (R) parameters for the  $(d,p)$  reaction was set to zero since it was not used in Refs. [8] and [9]. Including it in the calculations didn't significantly change the results.

Spectroscopic factors  $S$  can be determined by dividing the experimental cross-section  $\sigma_{(\text{Exp.})}$  by those obtained theoretically from DWBA calculations  $\sigma_{(\text{DWBA})}$  with CHUCK3:

$$\sigma_{(\text{Exp.})} = S * \sigma_{(\text{DWBA})}. \quad (2)$$

<sup>1</sup> Maier-Leibnitz Laboratory of the Technische Universität München and the Ludwig-Maximilians-Universität München

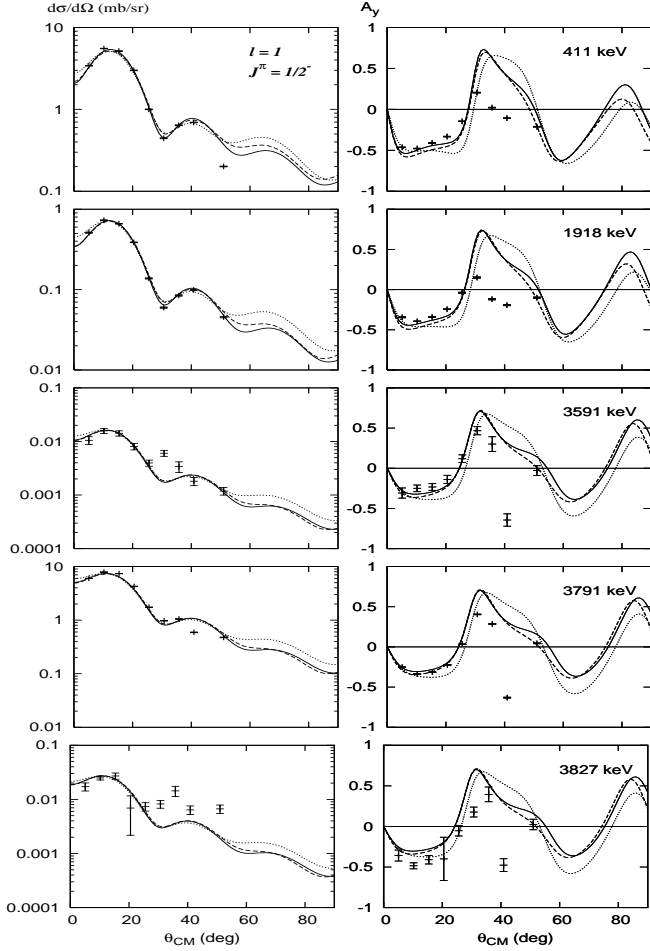


**Fig. 2.** Differential cross-section  $\frac{d\sigma}{d\Omega}$  and the analyzing power  $A_y$  for  $^{55}\text{Fe}$  levels with  $\Delta l = 1$  and  $J^\pi = 1/2^-$ . Curves indicate the DWBA calculations by CHUCK3 using the three different sets of OM-potentials from Refs.[18] (full curve), [9] (dotted curve) and [17] (dashed curve).

In our case,  $S$  was determined by a  $\chi^2$  fit to the angular distributions.

The agreement of calculated angular distributions and analyzing powers with the experimental data is quite satisfactory for the different sets of optical model parameters. One may argue that the description based on the parameters of Ref.[9] is slightly inferior. Tables 2 and 3 summarize the results for all observed levels in  $^{55}\text{Fe}$ . The excitation energies for those known levels that have uncertainties of less than 1 keV in Ref. [8] agreed for most states within less than 0.5 keV with the exceptions of the 2051.7 (4) keV, 2577.7(4) keV, and 3072.0(4) keV states for which energies of 2050.1(5) keV, 2579.2(5) keV and 3070.2(5) keV were measured in this work, respectively. Above 3.1 MeV we estimate the uncertainties of the measured energies to be 2 keV.

In total, 19 previous spin assignments could be confirmed and for six levels (2872, 3107, 3308, 3777, 3804, 4043 keV) with tentative or several possible spin assignments a firm spin and parity assignment could be made.

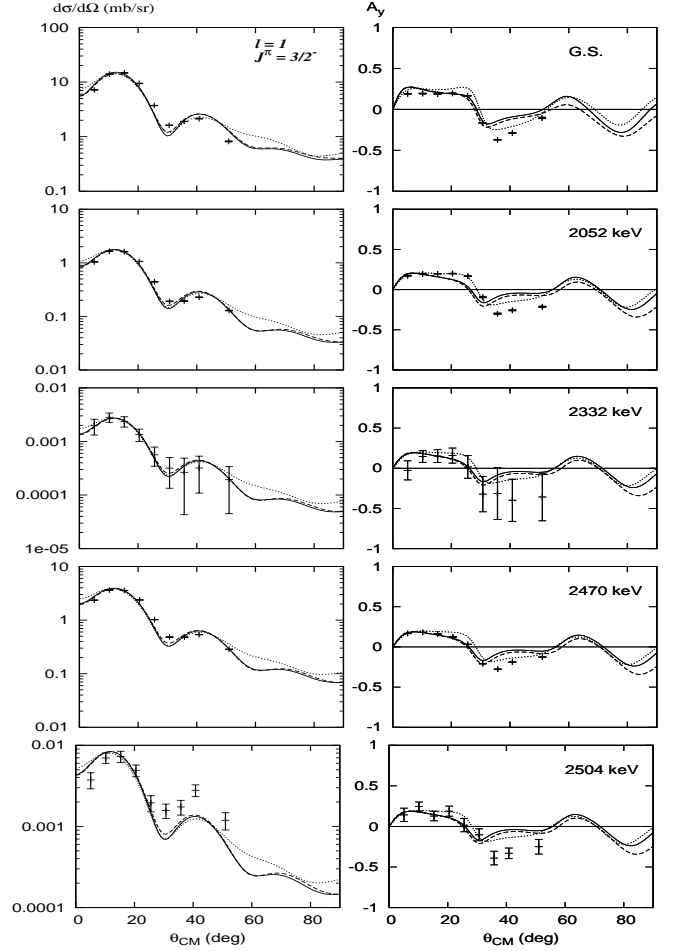


**Fig. 3.** Same as Fig. 2 for states with  $\Delta l = 1$  and  $J^\pi = 3/2^-$  and energies below 3.0 MeV.

For seven known levels (3354, 3655, 3716, 4019, 4117, 4134, 4372 keV) spin and parity were determined for the first time while seven levels (2332, 2504, 3576, 3827, 3939, 4260, 4292 keV) were newly observed. It was possible to obtain spectroscopic factors for all 39 observed levels, which are also listed in tables 2 and 3. The uncertainties given for the spectroscopic factors in tables 2 and 3 refer to the standard deviation of the three spectroscopic factor values obtained for the different optical model parameters. As can be easily seen, the  $S$ -values for the different optical model parameters differ only slightly. However, the cross sections may contain additional systematic uncertainties on the order of 10-20% mainly due to uncertainties in the target thickness. The absolute spectroscopic factors obtained in this work generally compare favorably with those previously reported [8,9]. If relative spectroscopic factors are considered, the agreement is even better.

Hereafter, the assignments for those levels will be discussed, for which the relation to known levels is not clear or where the assignment found in this work is in conflict with previous assignments.

*The 2212 keV level:* This level has a spin and parity assignment of  $J^\pi = \frac{9}{2}^-$  [8]. However, the agreement with

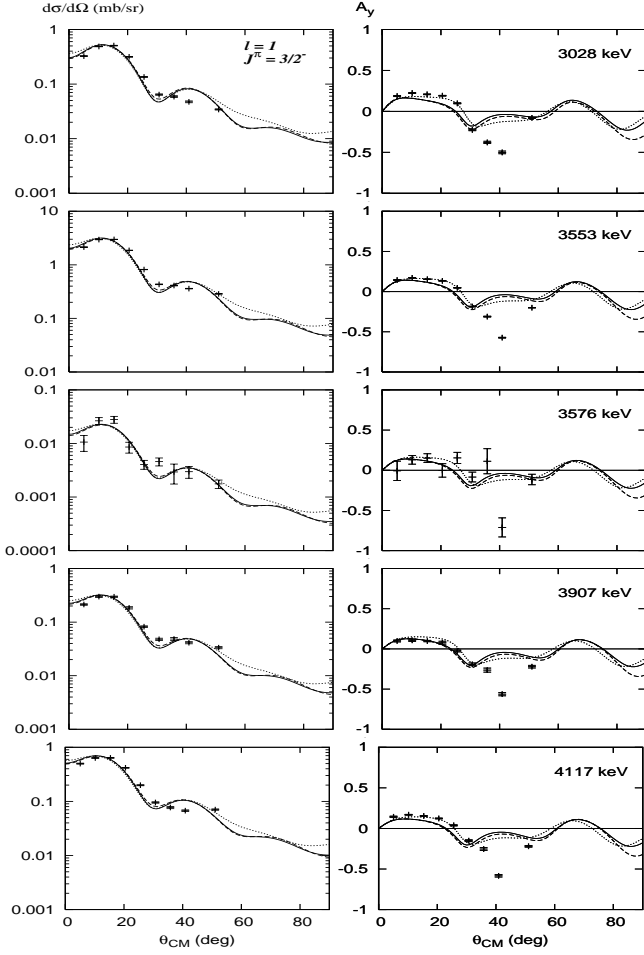


**Fig. 4.** Same as Fig. 2 for states with  $\Delta l = 1$  and  $J^\pi = 3/2^-$  and energies above 3.0 MeV.

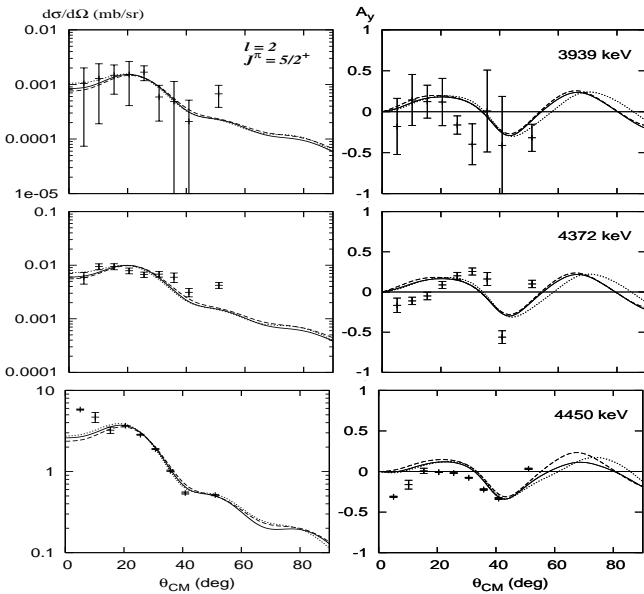


**Fig. 5.** Same as Fig. 2 for states with  $\Delta l = 2$  and  $J^\pi = 3/2^+$  and  $J^\pi = 5/2^+$ .

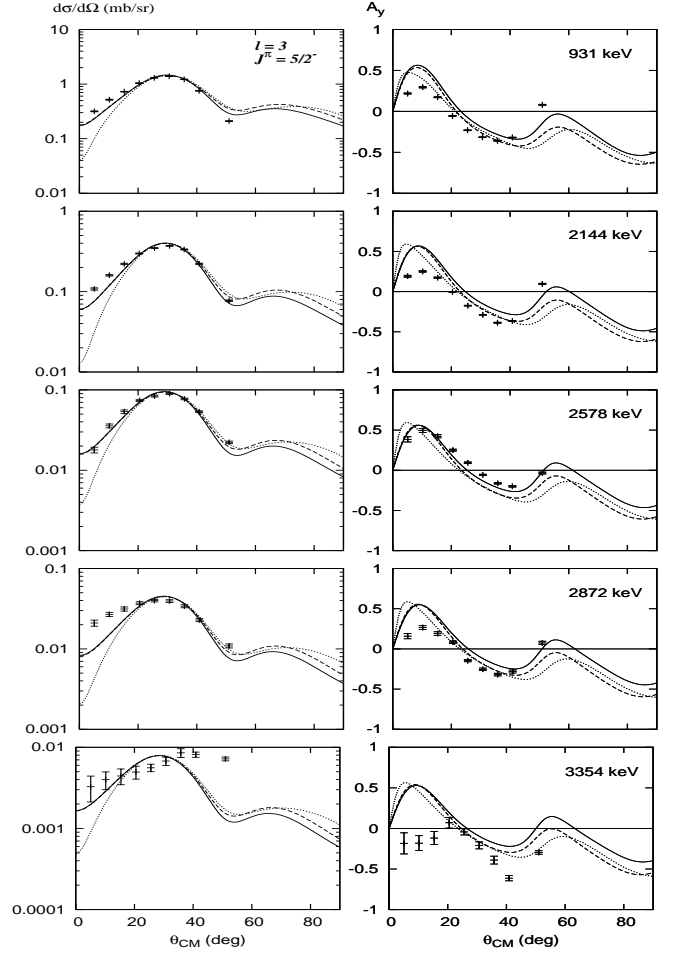


**Fig. 6.** Same as Fig. 2 for states with  $\Delta l = 3$  and  $J^\pi = 5/2^-$  and energies below 3.7 MeV.

the DWBA calculations for  $\Delta l = 5$  and  $J^\pi = \frac{9}{2}^-$  in fig. 10 is not really satisfactory. However, the measured cross section is less than 0.005 mb and multi-step processes may be important in this case.

*The 3070 keV level:* There is a 3072.0(4) keV state known with  $J^\pi = \frac{11}{2}^-$  [8], established from gamma-ray spectroscopy [20,21]. The measured angular distribution is rather flat, indicating a large angular momentum transfer and the analyzing power shows reasonable agreement with the  $J^\pi = \frac{11}{2}^-$  assignment. However, also in this case the level is populated very weakly and it is not possible to exclude multi-step processes. Therefore, a definite spin and parity assignment can not be made on the basis of the present data.

*The 3354 keV  $J^\pi = \frac{7}{2}^-$  level:* We associate this level with the 3362(10) keV level previously observed in the (d,p) study of Ref. [15].

*The 3591 keV  $J^\pi = \frac{1}{2}^-$  level:* We associate this level with the previously observed level at 3599(10) keV [8].

*The 3655 keV  $J^\pi = \frac{5}{2}^-$  level:* In Ref. [8] a level is reported at 3660.8(11) keV based on the observation of gamma rays populating this level following the  $^{51}\text{V}(^7\text{Li},3n)$

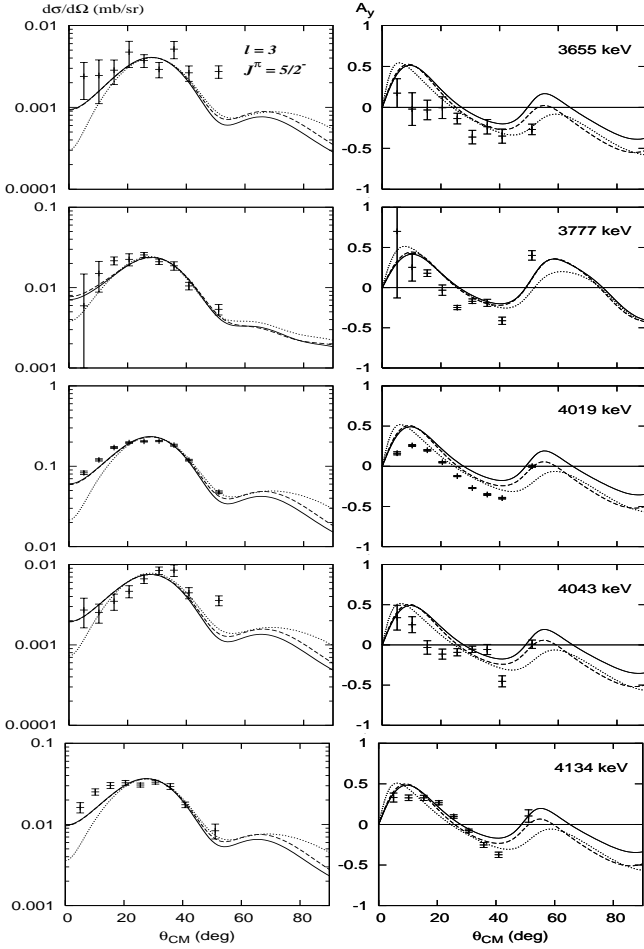


**Fig. 7.** Same as Fig. 2 for states with  $\Delta l = 3$  and  $J^\pi = 5/2^-$  and energies above 3.7 MeV.

reaction. In Ref. [8] this level is associated also with the 3661(10) keV level observed in (d,p) [15]. No spin and parity assignment was made for this level in either study. However, we do not observe a level at 3661 keV but rather at 3655(2) keV. Therefore, we suggest that there are two levels, one at 3660.8(11) keV and one at 3655(2) keV.

*The 3716 keV  $J^\pi = 7/2^-$  level:* A state at 3722(10) keV has been previously observed in (d,p) [8] but no  $J^\pi$  was assigned. We associate the 3716(2) keV level from this work with this state.

*The 3777 keV  $J^\pi = 5/2^-$  level:* A 3770 keV level was reported in (p,t) experiments and assigned as  $1/2^-$  [24] on the basis of observed  $\Delta l = 0$  angular distribution while in Ref. [23] a state at the same energy with  $\Delta l = 1, 2$  and possible spin assignments of  $(\frac{3}{2}^-, \frac{5}{2}^-)$  or  $(\frac{1}{2}^+, \frac{3}{2}^+)$  was reported. From the angular distribution and analyzing power of this level we clearly assign it as  $J^\pi = 5/2^-$ .

*The 3804 keV  $J^\pi = 9/2^+$  level:* Ref.[8] reports levels at 3814(10) keV  $(\frac{7}{2}^+, \frac{9}{2}^+)$ , and 3815(15)  $(\frac{5}{2}^-, \frac{7}{2}^-)$ . In earlier studies [15,7] a line doublet at 3.80 and 3.81 MeV was reported, which was analyzed in Ref. [7] by a superposition of two states with  $J^\pi = 1/2^-$  and  $J^\pi = (\frac{7}{2}^+, \frac{9}{2}^+)$ , re-

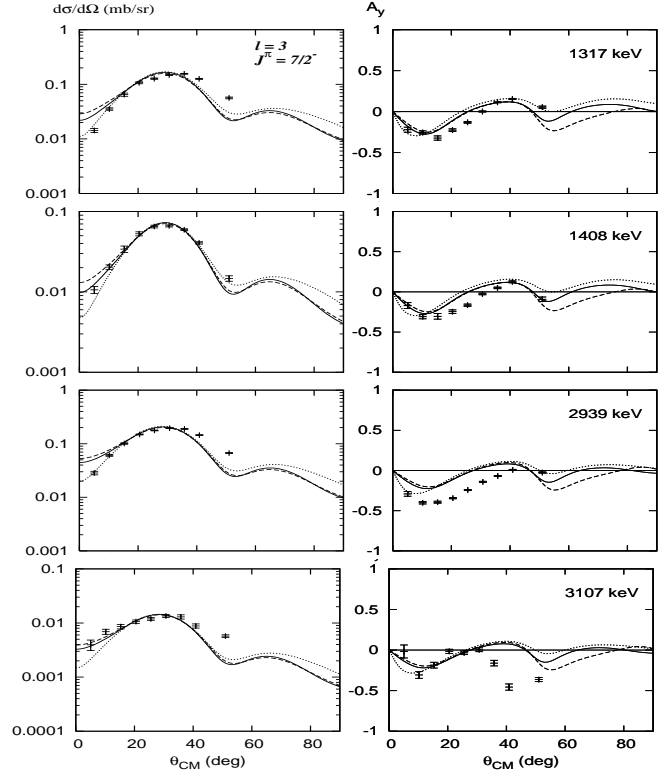


**Fig. 8.** Same as Fig. 2 for states with  $\Delta l = 3$  and  $J^\pi = 7/2^-$  and energies below 3.2 MeV.

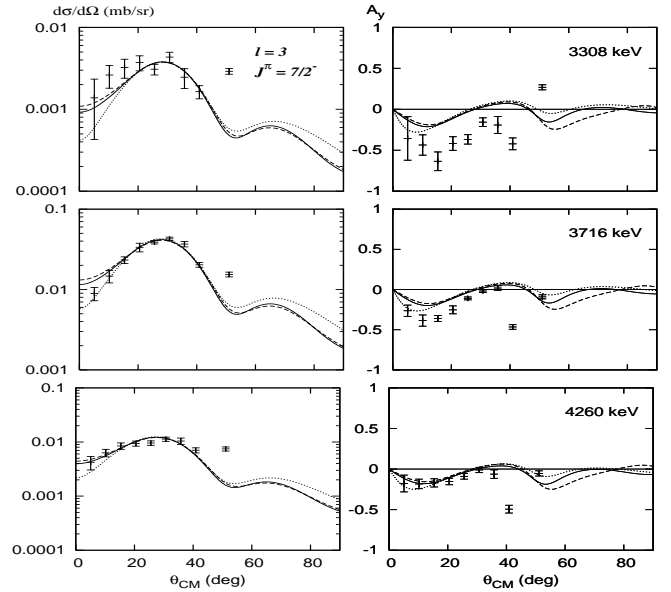


**Fig. 9.** Same as Fig. 2 for states with  $\Delta l = 3$  and  $J^\pi = 7/2^-$  and energies above 3.2 MeV.

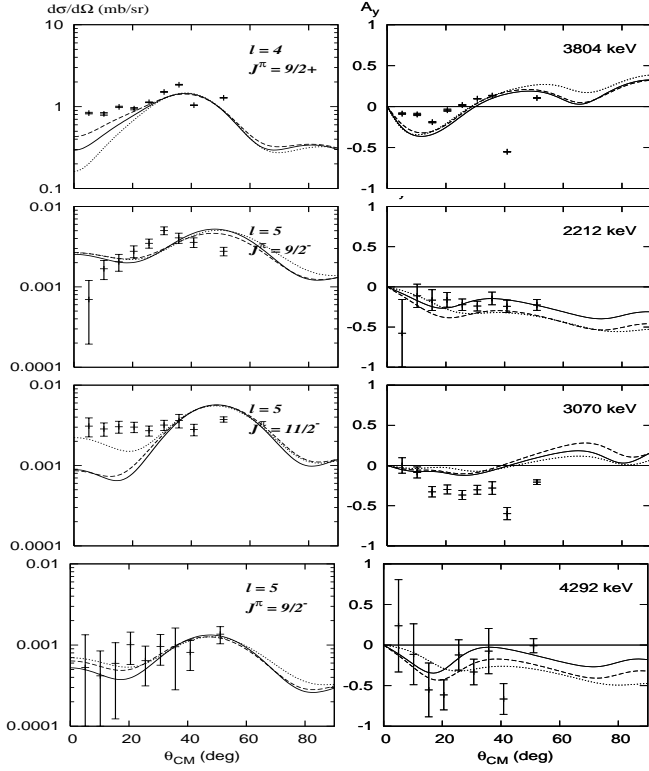


**Fig. 10.** Same as Fig. 2 for states with  $\Delta l = 4$  and  $\Delta l = 5$ .

**Table 1.** Optical-Model parameters for deuteron (D1[18],D2[9],D3[17]), proton (p) [18] and neutron (n) [18] for a beam energy of  $E_d^{\text{lab}} = 14$  MeV. V (W) denotes the real (imaginary) potentials with volume (vol.), surface (surf.) and spin-orbit (L.S.) terms, while r and a denote radius and diffuseness parameters.  $V_{\text{L.S.}}$  was taken from Ref. [17].

		Real			Imaginary		
		V (MeV)	$r_o$ (fm)	$a_o$ (fm)	W (MeV)	$r_I$ (fm)	$a_I$ (fm)
D1	vol.	-91.68	1.15	0.81			
	surf.				17.76	1.34	0.68
	L.S.	-6.92	1.07	0.66			
D2	vol.	-92.64	1.05	0.86			
	surf.				15.26	1.43	0.69
	L.S.	-7.00	0.75	0.5			
D3	vol.	-90.91	1.17	0.73	-0.25	1.33	0.74
	surf.				12.32	1.33	0.79
	L.S.	-6.92	0.75	0.5			
p	vol.	-53.16	1.17	0.75	-0.38	1.32	0.51
	surf.				8.75	1.32	0.51
	L.S.	-6.2	1.01	0.75			
n	vol.	1.00	1.17	0.75			
	L.S.	0.00	1.26	0.69			

**Table 2.** Transferred orbital angular momentum  $\Delta l$ , assigned total angular momentum and parity  $J^\pi$ , measured maximum differential cross section  $(\frac{d\sigma}{d\Omega})^{\text{max}}$  at center of mass angle  $\theta_{\text{max}}^{\text{cm}}$  as well as averaged absolute spectroscopic factors for the three optical model parameter sets from Refs. [18,9,17]. For comparison literature values for  $J_{\text{Lit.}}^\pi$  [8] and absolute spectroscopic factors  $S_{\text{Lit.}}$  are given. The uncertainties in the spectroscopic factors reflect the standard deviation of the three values over which was averaged. New levels are indicated with an asterisk. The uncertainties given for spectroscopic factors do not include additional systematic uncertainties of the cross-sections on the order of 10-20% mainly due to uncertainties in the target thickness.

$E_x^a$ [keV]	$\Delta l$	$J^\pi$ [ $\hbar$ ]	$J_{\text{Lit.}}^\pi$ [ $\hbar$ ]	$(\frac{d\sigma}{d\Omega})^{\text{max}}$ [ $\frac{\text{mb}}{\text{sr}}$ ]	$S_{\text{Aver.}}$	$S_{\text{Lit.}}$
0.0	1	$\frac{3}{2}^-$	$\frac{3}{2}^-$	14.67(2) 15.3	0.49(1)	0.575 <sup>b)</sup> 0.775 <sup>c)</sup>
411.0	1	$\frac{1}{2}^-$	$\frac{1}{2}^-$	5.53(5) 10.2	0.35(1)	0.30 <sup>b)</sup> 0.60 <sup>c)</sup>
931.4	3	$\frac{5}{2}^-$	$\frac{5}{2}^-$	1.39(1) 30.6	0.43(2)	0.35 <sup>b)</sup> 0.65 <sup>c)</sup>
1316.5	3	$\frac{7}{2}^-$	$\frac{7}{2}^-$	0.156(3) 35.7	0.028(1)	0.037 <sup>b)</sup> 0.045 <sup>c)</sup>
1408.2	3	$\frac{7}{2}^-$	$\frac{7}{2}^-$	0.066(2) 30.6	0.012(1)	0.015 <sup>b)</sup> 0.018 <sup>c)</sup>
1918.1	1	$\frac{1}{2}^-$	$\frac{1}{2}^-$	0.731(7) 10.2	0.0400(3)	0.04 <sup>b)</sup> 0.10 <sup>c)</sup>
2050.1	1	$\frac{3}{2}^-$	$\frac{3}{2}^-$	1.64(1) 10.2	0.046(1)	0.065 <sup>b)</sup> 0.088 <sup>c)</sup>
2144.0	3	$\frac{5}{2}^-$	$\frac{5}{2}^-$	0.371(4) 30.7	0.101(4)	0.098 <sup>b)</sup> 0.153 <sup>c)</sup>
2211.5	(5)	$(\frac{9}{2}^-)$	$\frac{9}{2}^-$	0.005(1) 30.7	0.0032(6)	
2332.2*	1	$\frac{3}{2}^-$		0.003(1) 10.2	0.00007(1)	
2470.2	1	$\frac{3}{2}^-$	$\frac{3}{2}^-$	3.65(2) 10.2	0.0963(2)	0.098 <sup>b)</sup> 0.17 <sup>c)</sup>
2503.8*	1	$\frac{3}{2}^-$		0.007(1) 15.3	0.00020(1)	
2579.2	3	$\frac{5}{2}^-$	$\frac{5}{2}^-$	0.090(2) 30.7	0.0224(9)	0.05 <sup>c)</sup> 0.03 <sup>d)</sup>
2872.3	3	$\frac{5}{2}^-$	$\frac{5}{2}^-$ , $\frac{7}{2}^-$	0.040(2) 25.6	0.0102(5)	
2938.9	3	$\frac{7}{2}^-$	$\frac{7}{2}^-$	0.195(3) 30.7	0.0280(5)	
3028.2	1	$\frac{3}{2}^-$	$\frac{3}{2}^-$	0.487(7) 10.2	0.0119(2)	0.021 <sup>d)</sup>
3070.2	(5)	$(\frac{11}{2}^-)$	$\frac{11}{2}^-$	0.004(1) 51.0	0.0031(5)	

<sup>a)</sup> Energies from this work with uncertainties of 0.5 keV. New levels are marked with \*.

<sup>b)</sup> Ref.[8]

<sup>c)</sup> Ref. [9]

<sup>d)</sup> Ref. [28]

spectively, consistent with our observation of the 3791(2) keV  $\frac{1}{2}^-$  and 3804(2) keV  $\frac{9}{2}^+$  levels observed in this work. The 3815(10) keV  $\frac{5}{2}^-, \frac{7}{2}^-$  level listed in the Nuclear Data Sheets [8] is supposedly observed in the ( $^3\text{He},\alpha$ ) reaction. However, the original work [22] only reports the 3814(20) keV  $\frac{9}{2}^+$  state. Therefore, one may come to the conclusion that the 3815(10) keV  $\frac{5}{2}^-, \frac{7}{2}^-$  level should be removed from the Nuclear Data Sheets.

*The 4019 keV  $J^\pi = \frac{5}{2}^-$  level:* We associate this level with the previously observed level at 4028(10) keV [8].

*The 4043 keV  $J^\pi = \frac{5}{2}^-$  level:* Ref.[8] reports a level at 4057(10) keV with the energy from [15] and a spectroscopic factor resulting from the averaged value of Refs. [7, 28]. However, Ref. [7] reports this ( $\frac{5}{2}^-$ ) level at 4.04 MeV while Ref. [28] reports it an energy of 4.039 MeV, both values consistent with our observation.

*The 4117 keV  $J^\pi = \frac{3}{2}^-$  level:* We associate this level with the previously observed level at 4110(10) keV [8].

*The 4134 keV  $J^\pi = \frac{5}{2}^-$  level:* We associate this level with the previously observed level at 4123(10) keV [8].

*The 4372 keV  $J^\pi = (\frac{5}{2}^+)$  level:* We associate this level with the previously observed level at 4372(10) keV [8]. Since the agreement of the experimental analyzing power with the DWBA results for a  $\frac{5}{2}^+$  state is not very good, we consider this assignment as tentative.

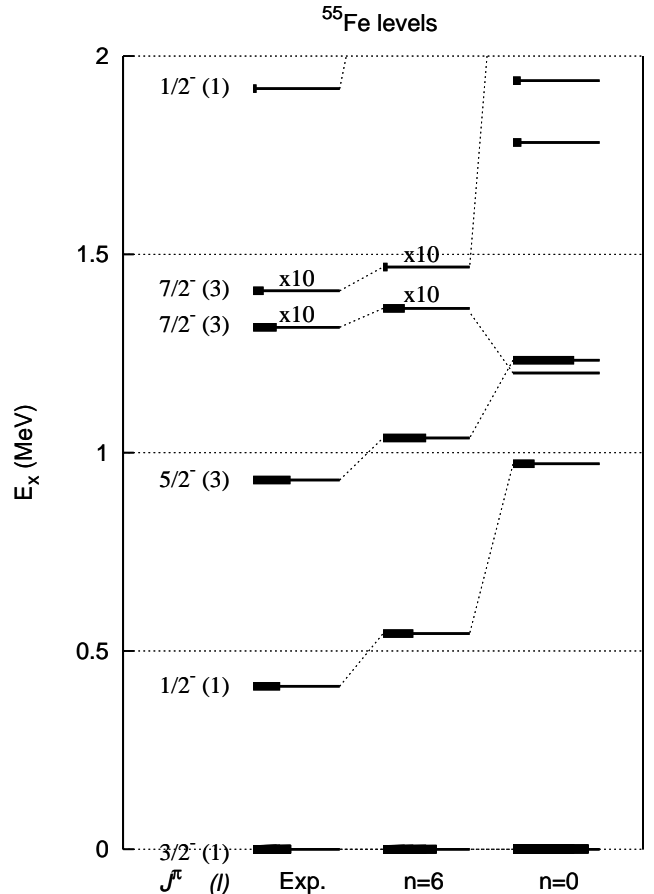
*The 4450 keV  $J^\pi = \frac{5}{2}^+$  level:* We associate this level with the previously observed  $\frac{5}{2}^+$  level at 4463(10) keV [8].

## 4 Discussion

The main aim of the current study was to investigate the role of cross-shell excitations for the  $N = 28$  shell gap in  $^{55}\text{Fe}$ . For this purpose we have performed large scale shell model calculations using the code ANTOINE [27] and employing the GXFP1 effective interaction [3,4] which was adjusted to the tremendous number of experimental data available for the pf-shell nuclei. The calculations were performed in the full pf-shell (*i.e.*,  $f_{7/2}$ ,  $p_{3/2}$ ,  $f_{5/2}$ , and  $p_{1/2}$  single-particle orbitals), with up to  $n = 6$  particles allowed to be excited from the  $f_{7/2}$  orbital to the  $p_{3/2}$ ,  $p_{1/2}$ , and  $f_{5/2}$  orbitals. Thus the 15-body wave function of  $^{55}\text{Fe}$ , corresponding to the space of valence nucleons, is a superposition of the  $(f_{7/2})^{(14-k)}(p_{3/2}p_{1/2}f_{5/2})^{1+k}$  components, where  $k$  is running from 0 (no cross-shell excitation) to  $n = 6$ . We have found that the agreement of the calculated level energies and spectroscopic factors with the experimental data improves with increasing  $n$  and the  $n = 6$  approximation (6p-6h) yields a reasonably good description of the experimental data. the spectroscopic factors for each  $n$  were calculated using the wave-function of the shell-model calculations for the same  $n$ . In this case the ground state of  $^{55}\text{Fe}$  contains only 57% of the wave function of the  $k = 0$  configuration. Also for all excited states the  $k = 0$  configuration is always less than 60%. It is interesting to note that the first excited  $\frac{7}{2}^-$  state contains only

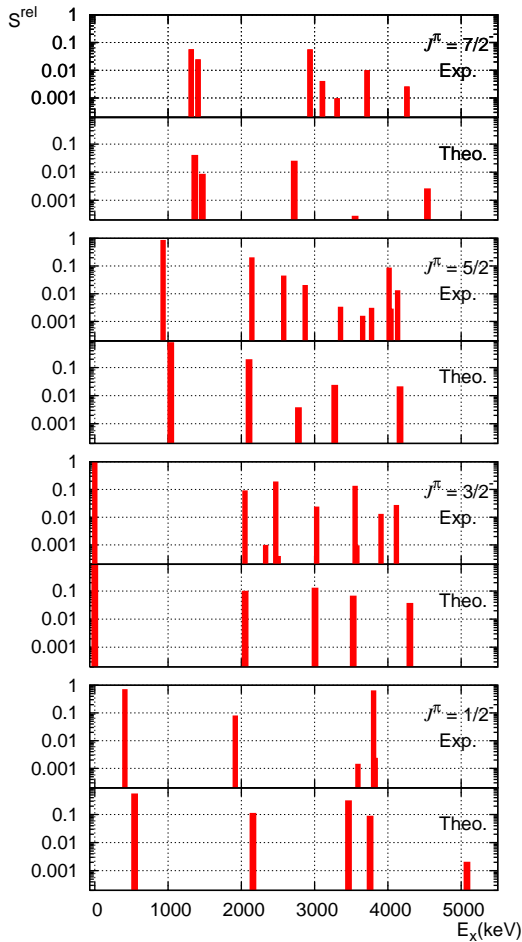
3% of the  $k = 0$  configuration (two proton holes in  $f_{7/2}$  shell) while the second  $\frac{7}{2}^-$  state contains a considerably larger fraction (47%) of the  $k = 0$  configuration. The calculated spectroscopic factor for the  $J^\pi = \frac{3}{2}^-$  ground state amounts to 0.87 in the  $n = 0$  case and reduces to 0.62 for  $n = 6$ , which is considerably closer to the experimental value of  $S = 0.49(1)$ .

Fig. 11 shows the energy levels below 2 MeV from shell model calculations for  $n = 0$  and  $n = 6$  in comparison with the experimental results. Also shown as horizontal bars are the absolute spectroscopic factors for the  $^{54}\text{Fe}(\vec{d},p)^{55}\text{Fe}$  reaction, where the full length of the thin level line corresponds to  $S = 1$ . For the two  $\frac{7}{2}^-$  levels the plotted spectroscopic factors are increased by a factor of 10 in order to enhance their visibility. We note that the agreement with the  $n = 6$  calculations is quite good, while the calculations based on an assumption of an inert  $N = 28$  core ( $n = 0$ ) fail to reproduce the experimental spectrum and spectroscopic factors even for the lowest states.



**Fig. 11.**  $^{55}\text{Fe}$  experimental levels compared to shell model predictions. Thick horizontal bars represent the absolute spectroscopic factors, with  $S = 1$  corresponding to the full length of the thin level line. The shell model results for  $n = 0$  and  $n = 6$  cases are labeled correspondingly.

The experimental and theoretical energies as well as relative spectroscopic factors for all  $J^\pi = \frac{1}{2}^-$ ,  $\frac{3}{2}^-$ ,  $\frac{5}{2}^-$ , and  $\frac{7}{2}^-$  levels up to an excitation energy of 5 MeV are compared in Fig. 12. We note that the agreement is very good below about 3 MeV for most spins. However, for the  $J^\pi = \frac{3}{2}^-$  states we observe already 3 levels more than we have obtained in the shell model calculation. Furthermore, the experimental strength is strongly fragmented already in the vicinity of 2.3 MeV. For other spin values we observe significantly more states and stronger fragmentation only above 3 MeV, with the exception of the  $J^\pi = \frac{1}{2}^-$  states. The above comparison clearly indicates that cross-shell excitations play an important role for the spectra and spectroscopic properties of low-lying states in  $^{55}\text{Fe}$ . Furthermore, to describe the experimentally observed density of states below 4-5 MeV one would need to go beyond the 6p-6h approximation adopted here and include higher np-nh excitations.



**Fig. 12.** Theoretical and experimental strength distribution of relative spectroscopic factors  $S^{\text{rel}}$ , normalized to the spectroscopic factor of the ground state  $J^\pi = \frac{3}{2}^-$ , for (from bottom to top)  $J^\pi = \frac{1}{2}^-$ ,  $J^\pi = \frac{3}{2}^-$ ,  $J^\pi = \frac{5}{2}^-$ , and  $J^\pi = \frac{7}{2}^-$  levels.

## 5 Summary

In a high resolution study of the reaction  $^{54}\text{Fe}(\vec{d},p)^{55}\text{Fe}$  39 levels were observed. On the basis of angular distributions and asymmetries firm spin and parity assignments could be made for all but 2 states, for which firm assignments were already available from previous studies. It was possible to observe eight new states and prove that five states previously assigned to  $^{55}\text{Fe}$  were actually states in  $^{57}\text{Fe}$ . For a number of known states energies could be determined with improved accuracy and spins were assigned for the first time. Spectroscopic factors were determined for all observed states. The results were compared with large scale shell model calculations using the GXPF1 effective interaction and good agreement was found up to 2 MeV when up to 6p-6h excitations across the  $N = 28$  shell were included, clearly establishing the significant role of cross-shell excitations in  $^{54}\text{Fe}$  and  $^{55}\text{Fe}$ . The observed larger number of levels and stronger fragmentation of the spectroscopic strength above 2.5 MeV in comparison to shell model results indicate that more many-body cross-shell degrees of freedom need to be taken into account to describe the experimental data obtained in this work.

## 6 Acknowledgement

The excellent work of the MLL accelerator crew is gratefully acknowledged. Useful discussions with J. Tostevin are acknowledged. This work was supported by DFG under grants KR2326/1-1, 436 RUM 17/1/07 and by the DFG cluster of excellence Origin and Structure of the Universe (<http://www.universe-cluster.de>). A.F.L. acknowledges partial support of this work from NSF grant PHY0555396.

## References

1. G. Kraus, P. Egelhof, C. Fischer, H. Geissel, A. Himmler, F. Nickel, G. Münzenberg, W. Schwab, A. Weiss, J. Friese, A. Gillitzer, H.J. Körner, M. Peter, W.F. Henning, J.P. Schiffer, J.V. Kratz, L. Chulkov, M. Golovkov, A. Ogloblin, B. A. Brown, Phys. Rev. Lett. 73, 1773 (1994).
2. T. Otsuka, M. Honma, T. Mizusaki, Phys. Rev. Lett. 81, 1588 (1998).
3. M. Honma, T. Otsuka, B.A. Brown, T. Mizusaki, Phys. Rev. C65, 061301 (2002).
4. M. Honma, T. Otsuka, B.A. Brown, T. Mizusaki, Phys. Rev. C69, 034335 (2004).
5. A.F. Lisetskiy, N. Pietralla, M. Honma, A. Schmidt, I. Schneider, A. Gade, P. von Brentano, T. Otsuka, T. Mizusaki, and B.A. Brown, Phys. Rev. C 68, 034316 (2003).
6. K. Langanke, G. Martinez-Pinedo, Rev. Mod. Phys. 75, 819 (2003).
7. D.C. Kocher, W. Haerberli, Nucl. Phys. A196, 225 (1972).
8. H. Junde Nucl. Data Sheets 109, 787 (2008).
9. T. Taylor and J.A. Cameron, Nuc. Phy. A337 (1980) 389.
10. R. Hertenberger, A. Metz, Y. Eisermann, K. El Abiary, A. Ludewig, C. Pertl, S. Trieb, H.-F. Wirth, P. Schiemenz, G. Graw, Nucl. Instr. Meth. A536, 266 (2005).



11. M. Löffler, H.J. Scheerer, H. Vonach, Nucl. Instrum. Methods 111, 1 (1973).
12. H.-F. Wirth, H. Angerer, T. von Egidy, Y. Eisermann, G. Graw, R. Hertenberg, Beschleunigerlaboratorium München Annual Report, 2000, p. 71.
13. H.-F. Wirth, PhD Thesis, Technische Universität München, 2001 (<http://tumb1.biblio.tu-muenchen.de/publ/diss/ph/2001/wirth01.pdf>).
14. M.H. Macfarlane and J.B. French Rev. Mod. Phys. 32 (1960) 567.
15. A. Sperduto and W.W. Buechner, Phys. Rev. 134 (1964) B142.
16. P.D. Kunz, Computer code CHUCK3, University of Colorado, unpublished.
17. H. Feshbach, Theoretical Nuclear Physics (Wiley, New York u.a. 1992).
18. C.M. Perey and F.G. Perey, Atom. Data and Nuc. Data. Tables 17 (1976) 1.
19. J.H. Polane, W.F. Feix, P.J. van Hall, S.S. Klein, G.J. Nijgh, O.J. Poppema, S.D. Wassenaar, J. Phys. G 15, 1735 (1989).
20. Z.P. Sawa, Phys. Scr. 6, 11 (1972).
21. A.R. Poletti, B.A. Brown, D.B. Fossan, E.K. Warburton, Phys. Rev. C 10, 2312 (1974).
22. M.A. Zaman, H.M. Sen Gupta, J. Phys. G 6, 1119 (1980).
23. R.J. Peterson, H. Rudolph, Nucl. Phys. A191, 47 (1972).
24. J.R. Maxwell, G.M. Reynolds, N.M. Hintz, Phys. Lett. 22, 454 (1966).
25. E.I. Firsov, N.G. Loskutova, E.A. Rudak, Nucl. Phys. 73, 312 (1965).
26. D.S. Gemmel, L.L. Lee, Jr., A. Marinov, J.P. Schiffer, Phys. Rev. 144, 923 (1966).
27. E. Caurier and F. Nowacki, Acta Phys. Pol. B 30, 705 (1999).
28. R.H. Fulmer and A.L. McCarthy, Phys. Rev. 131, 2133 (1963).

**Table 3.** Same as Tab.2 for states above 3.1 MeV.

$E_x^a)$ [keV]	$\Delta I$ [ $\hbar$ ]	$J^\pi$ [ $\hbar$ ]	$J_{\text{Lit.}}^\pi$ [ $\hbar$ ]	$(\frac{d\sigma}{d\Omega})_{\text{max}}^{\text{cm}}$ [ $\frac{\text{mb}}{\text{sr}}$ ]	$S_{\text{Aver.}}$	$S_{\text{Lit.}}$
3107	3	$\frac{7}{2}^-$	$\frac{5}{2}^-, \frac{7}{2}^-$	0.013(1) 30.7	0.0020(1)	
3308	3	$\frac{7}{2}^-$	$\frac{5}{2}^-, \frac{7}{2}^-$	0.004(1) 30.7	0.00048(2)	
3354	3	$\frac{5}{2}^-$		0.009(1) 35.8	0.0017(1)	
3553	1	$\frac{3}{2}^-$	$\frac{3}{2}^-$	2.982(25) 15.4	0.0671(1)	0.085 <sup>b)</sup> 0.12 <sup>c)</sup>
3576*	1	$\frac{3}{2}^-$		0.028(4) 15.4	0.00048(2)	
3591	1	$\frac{1}{2}^-$	$\frac{1}{2}^-$	0.016(2) 10.2	0.00072(2)	
3655	3	$\frac{5}{2}^-$		0.005(1) 35.8	0.00080(5)	
3716	3	$\frac{7}{2}^-$		0.043(2) 30.7	0.0050(1)	
3777	3	$\frac{5}{2}^-$	$\frac{3}{2}^-, \frac{5}{2}^-$ e) $\frac{1}{2}^+, \frac{3}{2}^+$ e) $\frac{1}{2}^-$ f)	0.025(2) 25.6 25.6	0.00155(4)	
3791	1	$\frac{1}{2}^-$	$\frac{1}{2}^-$	7.87(6) 10.2	0.3208(6)	0.5 <sup>c)</sup> $\approx 0.7^g)$
3804	4	$\frac{9}{2}^+$	$\frac{7}{2}^+, \frac{9}{2}^+$	1.85(2) 35.8	0.2734(7)	
3827*	1	$\frac{1}{2}^-$		0.027(4) 15.4	0.00117(3)	
3907	1	$\frac{3}{2}^-$	$\frac{3}{2}^-$	0.299(11) 10.2	0.0065(1)	0.018 <sup>g)</sup>
3939*	2	$(\frac{5}{2}^+)$		0.002(1) 25.6	0.00004(1)	
4019	3	$\frac{5}{2}^-$		0.206(4) 30.7	0.043(2)	0.06 <sup>c)</sup>
4043	3	$\frac{5}{2}^-$	$\frac{5}{2}^-, \frac{7}{2}^-$	0.009(1) 35.8	0.00140(3)	0.056 <sup>g)</sup>
4117	1	$\frac{3}{2}^-$		0.636(9) 15.4	0.0137(2)	
4134	3	$\frac{5}{2}^-$		0.033(2) 30.7	0.0066(3)	
4260*	3	$\frac{7}{2}^-$		0.011(1) 30.7	0.00130(2)	
4292*	5	$\frac{9}{2}^-$		0.001(0) 51.1	0.0008(1)	
4372	2	$(\frac{5}{2}^+)$		0.009(1) 15.4	0.00022(1)	
4450	2	$\frac{5}{2}^+$	$\frac{5}{2}^+$	5.80(9) 5.1	0.24(2)	0.13 <sup>c)</sup> 0.17 <sup>g)</sup>

<sup>a)</sup> Energies from this work with uncertainties of 2 keV. New levels are marked with \*.

<sup>b)</sup> Ref. [8]

<sup>c)</sup> Ref. [9]

<sup>d)</sup> Ref. [7]

<sup>e)</sup> Ref. [23]

<sup>f)</sup> Ref. [24]

<sup>g)</sup> Ref. [28]